1   SARS-CoV-2 mRNA Vaccine Development Enabled by Prototype Pathogen Preparedness

2

3   Kizzmekia S. Corbett[1#], Darin Edwards[2#], Sarah R. Leist[3#], Olubukola M. Abiona[1], Seyhan

4   Boyoglu-Barnum[1], Rebecca A. Gillespie[1], Sunny Himansu[2], Alexandra Schäfer[3], Cynthia T.

5   Ziwawo[1], Anthony T. DiPiazza[1], Kenneth H. Dinnon[3], Sayda M. Elbashir[2], Christine A. Shaw[2],

6   Angela Woods[2], Ethan J. Fritch[4], David R. Martinez[3], Kevin W. Bock[5], Mahnaz Minai[5], Bianca

7   M. Nagata[5], Geoffrey B. Hutchinson[1], Kapil Bahl[2], Dario Garcia-Dominguez[2], LingZhi Ma[2],

8   Isabella Renzi[2], Wing-Pui Kong[1], Stephen D. Schmidt[1], Lingshu Wang[1], Yi Zhang[1], Laura J.

9   Stevens[6], Emily Phung[7], Lauren A. Chang[1], Rebecca J. Loomis[1], Nedim Emil Altaras[2], Elisabeth

10   Narayanan[2], Mihir Metkar[2], Vlad Presnyak[2], Catherine Liu[1], Mark K. Louder[1], Wei Shi[1],

11   Kwanyee Leung[1], Eun Sung Yang[1], Ande West[3], Kendra L. Gully[3], Nianshuang Wang[8], Daniel

12   Wrapp[8], Nicole A. Doria-Rose[1], Guillaume Stewart-Jones[2], Hamilton Bennett[2], Martha C.

13   Nason[9], Tracy J. Ruckwardt[1], Jason S. McLellan[8], Mark R. Denison[6], James D. Chappell[6], Ian

14   N. Moore[5], Kaitlyn M. Morabito[1], John R. Mascola[1], Ralph S. Baric[3,4], Andrea Carfi[2*], Barney S.

15   Graham[1*]

16

17   #Authors have equal contribution to this study

18

19   [1]Vaccine Research Center; National Institute of Allergy and Infectious Diseases; National

20   Institutes of Health; Bethesda, Maryland, 20892; United States of America

21   [2]Moderna Inc., Cambridge, MA, 02139; United States of America

22   [3]Department of Epidemiology; University of North Carolina at Chapel Hill; Chapel Hill, North

23   Carolina, 27599; United States of America

24   [4]Department of Microbiology and Immunology, School of Medicine, University of North Carolina

25   at Chapel Hill; Chapel Hill, North Carolina, 27599; United States of America

26 [5]National Institute of Allergy and Infectious Diseases; National Institutes of Health; Bethesda,

27 Maryland, 20892; United States of America

28 [6]Department of Pediatrics, Vanderbilt University Medical Center, Nashville, Tennessee, 37212;

29 United States of America

30 [7]Institute for Biomedical Sciences, George Washington University, Washington, DC 20052,

31 United States of America

32 [8]Department of Molecular Biosciences; University of Texas at Austin; Austin, Texas, 78712;

33 United States of America

34 [9]Biostatistics Research Branch, Division of Clinical Research, National Institute of Allergy and

35 Infectious Diseases, National Institutes of Health; Bethesda, Maryland, 20892; United States of

36 America

37

38 *Correspondence: bgraham@nih.gov; Andrea.Carfi@modernatx.com

39 **Summary**

40 A SARS-CoV-2 vaccine is needed to control the global COVID-19 public health crisis. Atomic-

41 level structures directed the application of prefusion-stabilizing mutations that improved

42 expression and immunogenicity of betacoronavirus spike proteins. Using this established

43 immunogen design, the release of SARS-CoV-2 sequences triggered immediate rapid

44 manufacturing of an mRNA vaccine expressing the prefusion-stabilized SARS-CoV-2 spike

45 trimer (mRNA-1273). Here, we show that mRNA-1273 induces both potent neutralizing antibody

46 and CD8 T cell responses and protects against SARS-CoV-2 infection in lungs and noses of

47 mice without evidence of immunopathology. mRNA-1273 is currently in a Phase 2 clinical trial

48 with a trajectory towards Phase 3 efficacy evaluation.

49   Since its emergence in December 2019, severe acute respiratory syndrome coronavirus 2

50   (SARS-CoV-2) has accounted for over 7 million cases of Coronavirus Disease 2019 (COVID-

51   19) worldwide in less than 7 months[1]. SARS-CoV-2 is the third novel betacoronavirus in the last

52   20 years to cause substantial human disease; however, unlike its predecessors SARS-CoV and

53   MERS-CoV, SARS-CoV-2 transmits efficiently from person-to-person. In absence of a vaccine,

54   public health measures such as quarantining newly diagnosed cases, contact tracing, and

55   mandating face masks and physical distancing have been instated to reduce transmission[2]. It is

56   estimated that until 60-70% population immunity is established, it is unlikely for COVID-19 to be

57   controlled well enough to resume normal activities. If immunity remains solely dependent on

58   infection, even at a 1% mortality rate, >40 million people could succumb to COVID-19 globally[3].

59   Therefore, rapid development of vaccines against SARS-CoV-2 is critical for changing the

60   global dynamic of this virus.

61   The spike (S) protein, a class I fusion glycoprotein analogous to influenza hemagglutinin (HA),

62   respiratory syncytial virus (RSV) fusion glycoprotein (F), and human immunodeficiency virus

63   (HIV) gp160 (Env), is the major surface protein on the CoV virion and the primary target for

64   neutralizing antibodies. S proteins undergo dramatic structural rearrangement to fuse virus and

65   host cell membranes, allowing delivery of the viral genome into target cells. We previously

66   showed that prefusion-stabilized protein immunogens that preserve neutralization-sensitive

67   epitopes are an effective vaccine strategy for enveloped viruses, such as RSV[4-8]. Subsequently,

68   we identified 2 proline substitutions (2P) at the apex of the central helix and heptad repeat 1 that

69   effectively stabilized MERS-CoV, SARS-CoV and HCoV-HKU1 S proteins in the prefusion

70   conformation[9-11]. Similar to other prefusion-stabilized fusion proteins, MERS S-2P protein is

71   more immunogenic at lower doses than wild-type S protein[11]. The 2P has been widely

72   transferrable to other beta-CoV spike proteins, suggesting a generalizable approach for

73   designing stabilized prefusion beta-CoV S vaccine antigens. This is fundamental to the

74   prototype pathogen approach for pandemic preparedness[12,13].

75   Coronaviruses have long been predicted to have a high likelihood of spill over into humans and

76   cause future pandemics[14,15]. As part of our pandemic preparedness efforts, we have studied

77   MERS-CoV as prototype pathogen for betacoronaviruses to optimize vaccine design, to dissect

78   the humoral immune response to vaccination, and identify mechanisms and correlates of

79   protection. Achieving an effective and rapid vaccine response to a newly emerging virus

80   requires the precision afforded by structure-based antigen design but also a manufacturing

81   platform to shorten time to product availability. Producing cell lines and clinical grade subunit

82   protein typically takes more than 1 year, while manufacturing nucleic acid vaccines can be done

83   in a matter of weeks[16,17]. In addition to advantages in manufacturing speed, mRNA vaccines are

84   potently immunogenic and elicit both humoral and cellular immunity[18-20]. Therefore, we

85   evaluated mRNA formulated in lipid nanoparticles (mRNA/LNP) as a delivery vehicle for the

86   MERS S-2P and found that transmembrane-anchored MERS S-2P mRNA elicited better

87   neutralizing antibody responses than secreted MERS S-2P **(Extended Data Fig. 1a)**.

88   Additionally, consistent with protein immunogens, MERS S-2P mRNA was more immunogenic

89   than MERS wild-type S mRNA **(Extended Data Fig. 1b).** Immunization with MERS S-2P

90   mRNA/LNP elicited potent neutralizing activity down to a 0.1 µg dose and protected hDPP4

91   transgenic ($288/330^{+/+21}$) mice against lethal MERS-CoV challenge in a dose-dependent

92   manner, establishing proof-of-concept that mRNA expressing the stabilized S-2P protein is

93   protective. Notably, the sub-protective 0.01 µg dose of MERS S-2P mRNA did not cause

94   exaggerated disease following MERS-CoV infection, but instead resulted in partial protection

95   against weight loss followed by full recovery without evidence of enhanced illness **(Fig. 1)**.

96   In early January 2020, a novel CoV (nCoV) was identified as the cause of a respiratory virus

97   outbreak occurring in Wuhan, China. Within 24 hours of the release of the SARS-CoV-2 isolate

98   sequences (then known as "2019-nCoV") on January 10th, the 2P mutations were substituted

99   into S positions aa986 and 987 to produce prefusion-stabilized SARS-CoV-2 S (S-2P) protein

100   for structural analysis[22] and serological assay development[23,24] *in silico* without additional

101   experimental validation. Within 5 days of sequence release, current Good Manufacturing

102   Practice (cGMP) production of mRNA/LNP expressing the SARS-CoV-2 S-2P as a

103   transmembrane-anchored protein with the native furin cleavage site (mRNA-1273) was initiated

104   in parallel with preclinical evaluation. Remarkably, this led to the start of a first in human Phase

105   1 clinical trial on March 16, 2020, 66 days after the viral sequence was released, and a Phase 2

106   began 74 days later on May 29, 2020 **(Extended Data Fig. 2)**. Prior to vaccination of the first

107   human subject, expression and antigenicity of the S-2P antigen delivered by mRNA was

108   confirmed *in vitro* **(Extended Data Fig. 3),** and immunogenicity of mRNA-1273 was

109   documented in several mouse strains. The results of those studies are detailed hereafter.

110   Immunogenicity was assessed in six-week old female BALB/cJ, C57BL/6J, and B6C3F1/J mice

111   by immunizing intramuscularly (IM) twice with 0.01, 0.1, or 1 µg of mRNA-1273 at a 3-week

112   interval. mRNA-1273 induced dose-dependent S-specific binding antibodies after prime and

113   boost in all mouse strains **(Fig. 2a-c)**. Potent neutralizing activity was elicited by 1 µg of mRNA-

114   1273, reaching 819, 89, and 1115 reciprocal IC_{50} geometric mean titer (GMT) for BALB/cJ,

115   C57BL/6J, and B6C3F1/J mice, respectively **(Fig. 2d-f)**. These levels are similar to the

116   neutralization activity achieved by immunizing with 1 µg of SAS-adjuvanted S-2P protein

117   **(Extended Data Table 1)**. To further gauge immunogenicity across a wide dose range,

118   BALB/cJ mice were immunized with 0.0025 – 20 µg of mRNA-1273 revealing a strong positive

119   correlation between dose-dependent mRNA-1273-elicited binding and neutralizing antibody

120   responses **(Extended Data Fig. 4)**. BALB/cJ mice that received a single dose of mRNA-1273

121   were evaluated in order to ascertain the utility for a one-dose vaccine regimen. S-binding

122   antibodies were induced in mice immunized with one dose of 1 or 10 µg of mRNA-1273, and the

123   10 µg dose elicited neutralizing antibody activity that increased between week 2 and week 4,

124   reaching 315 reciprocal IC_{50} GMT **(Extended Data Fig. 5a-b)**. These data demonstrate that

125   mRNA expressing SARS-CoV-2 S-2P is a potent immunogen and neutralizing activity can be

126   elicited with a single dose.

127   Next, we evaluated the balance of Th1 and Th2, because vaccine-

128   associated enhanced respiratory disease (VAERD) has been associated with Th2-biased

129   immune responses in children immunized with whole-inactivated virus vaccines against RSV

130   and measles virus[25,26]. A similar phenomenon has also been reported in some animal models

131   with whole-inactivated SARS-CoV vaccines[27]. Thus, we first compared levels of S-specific

132   IgG2a/c and IgG1, which are surrogates of Th1 and Th2 responses respectively, elicited by

133   mRNA-1273 to those elicited by SARS-CoV-2 S-2P protein adjuvanted with the TLR4-agonist

134   Sigma Adjuvant System (SAS). Both immunogens elicited IgG2a and IgG1 subclass S-binding

135   antibodies, indicating a balanced Th1/Th2 response **(Fig. 3a-c; Extended Data Fig. 6)**. The S-

136   specific IgG subclass profile following a single dose of mRNA-1273 (**Extended Data Fig. 5c**)

137   was similar to that observed following two doses. In contrast, Th2-biased antibodies with lower

138   IgG2a/IgG1 subclass response ratios were observed in mice immunized with SARS-CoV-2 S

139   protein formulated in alum **(Extended Data Fig. 7a-b).** Following re-stimulation with peptide

140   pools (S1 and S2) corresponding to the S protein, splenocytes from mRNA-1273-immunized

141   mice secreted more IFN-γ than IL-4, IL-5, or IL-13 whereas SARS-CoV-2 S protein with alum

142   induced Th2-skewed cytokine secretion **(Extended Data Fig. 7c-d)**. 7 weeks post-boost, we

143   also directly measured cytokine patterns in vaccine-induced memory T cells by intracellular

144   cytokine staining (ICS); mRNA-1273-elicited CD4+ T cells re-stimulated with S1 or S2 peptide

145   pools exhibited a Th1-dominant response, particularly at higher immunogen doses **(Fig. 3d-e)**.

146   Furthermore, 1 µg of mRNA-1273 induced a robust CD8+ T cell response to the S1 peptide pool

147   **(Fig. 3f-g)**. The Ig subclass and T cell cytokine data together demonstrate that immunization

148   with mRNA-1273 elicits a balanced Th1/Th2 response in contrast to the Th2-biased response

149   seen with S protein adjuvanted with alum, suggesting that mRNA vaccination avoids Th2-biased

150   immune responses that have been linked to VAERD.

151   Protective immunity was assessed in young adult BALB/cJ mice challenged with mouse-

152   adapted (MA) SARS-CoV-2 that exhibits viral replication localized to lungs and nasal

153   turbinates[28]. BALB/cJ mice that received two 1 μg doses of mRNA-1273 were completely

154   protected from viral replication in lungs after challenge at a 5- **(Fig. 4a)** or 13-week intervals

155   following boost **(Extended Data Fig. 8a)**. mRNA-1273-induced immunity also rendered viral

156   replication in nasal turbinates undetectable in 6 out of 7 mice **(Fig. 4b, Extended Data Fig. 8b)**.

157   Efficacy of mRNA-1273 was dose-dependent, with two 0.1 μg mRNA-1273 doses reducing lung

158   viral load by ~100-fold and two 0.01 μg mRNA-1273 doses reducing lung viral load by ~3-fold

159   **(Fig. 4a)**. Of note, mice challenged 7 weeks after a single dose of 1 μg or 10 μg of mRNA-1273

160   were also completely protected against lung viral replication **(Fig. 4c).** Challenging animals

161   immunized with sub-protective doses provides an orthogonal assessment of safety signals,

162   such as increased clinical illness or pathology. Similar to what was observed with MERS-CoV S-

163   2P mRNA, mice immunized with sub-protective 0.1 and 0.01 μg mRNA-1273 doses showed no

164   evidence of enhanced lung pathology or excessive mucus production **(Fig. 4d)**. In summary,

165   mRNA-1273 is immunogenic, efficacious, and does not show evidence of promoting VAERD

166   when given at sub-protective doses in mice.

167   Here, we showed that 1 μg of mRNA-1273 was sufficient to induce robust neutralizing activity

168   and CD8 T cell responses, balanced Th1/Th2 antibody isotype responses, and protection from

169   viral replication for more than 3 months following a prime/boost regimen similar to that being

170   tested in humans. Inclusion of lower sub-protective doses demonstrated the dose-dependence

171   of antibody, Th1 CD4 T cell responses, and protection, suggesting immune correlates of

172   protection can be further elucidated. A major goal of animal studies to support SARS-CoV-2

173   vaccine candidates through clinical trials is to not only prove elicitation of potent protective

174   immune responses, but to show that sub-protective responses do not cause VAERD[3]. Sub-

175   protective doses did not prime mice for enhanced immunopathology following challenge.

176   Moreover, the induction of protective immunity following a single dose suggests that

177   consideration could be given to administering one dose of this vaccine in the outbreak setting.

178   These data, combined with immunogenicity data from nonhuman primates and subjects in early

179   Phase 1 clinical trials, will be used to inform the dose and regimen of mRNA-1273 in advanced

180   clinical efficacy trials.

181   The COVID-19 pandemic of 2020 is the Pathogen X event that has long been predicted[12,13].

182   Here, we provide a paradigm for rapid vaccine development. Structure-guided stabilization of

183   the MERS-CoV S protein combined with a fast, scalable, and safe mRNA/LNP vaccine platform

184   led to a generalizable beta-CoV vaccine solution that translated into a commercial mRNA

185   vaccine delivery platform, paving the way for the rapid response to the COVID-19 outbreak. This

186   is a demonstration of how the power of new technology-driven concepts like synthetic

187   vaccinology facilitate a vaccine development program that can be initiated with pathogen

188   sequences alone[11]. It is also a proof-of-concept for the prototype pathogen approach for

189   pandemic preparedness and response that is predicated on identifying generalizable solutions

190   for medical countermeasures within virus families or genera[12]. Even though the response to the

191   COVID-19 pandemic is unprecedented in its speed and breadth, we envision a response that

192   could be quicker. There are 24 other virus families known to infect humans, and with sustained

193   investigation of those potential threats, we could be better prepared for future looming

194   pandemics[13].

195

196   **Acknowledgements**

214

215   Author Contributions

216   K.S.C., D.K.E., S.R.L., O.M.A, S.B.B., R.A.G., S.H., A.S., C.Z., A.T.D., K.H.D., S.E., C.A.S.,

217   A.W., E.J.F., D.R.M, K.W.B., M.M., B.M.N., G.B.H., K.B., D.G.D., L.M., I.R., W.P.K, S.S., L.W.,

218   Y.Z., J.C., L.S., L.A.C., E.P., R.J.L., N.E.A., E.N., M.M., V.P., C.L., M.K.L., W.S., K.G., K.L.,

219   E.S.Y., A.W., G.A., N.A.D.R., G.S.J., H.B., M.N., T.J.R., M.R.D., I.N.M., K.M.M., J.R.M., R.S.B.,

220   A.C., and B.S.G. designed, completed, and/or analyzed experiments. N.W., D.W., and J.S.M.

221   contributed new reagents/analytic tools. K.S.C., K.M.M, and B.S.G. wrote the manuscript. All

222   authors contributed to discussions in regard to and editing of the manuscript.

223

Competing Interest Declaration

225 K.S.C., N.W., J.S.M., and B.S.G. are inventors on International Patent Application No.

226 WO/2018/081318 entitled "Prefusion Coronavirus Spike Proteins and Their Use." K.S.C., O.M.A.,

227 G.B.H., N.W., D.W., J.S.M, and B.S.G. are inventors on US Patent Application No. 62/972,886

228 entitled "2019-nCoV Vaccine". R.S.B. filed an invention report for the SARS-CoV-2 MA virus

229 (UNC ref. #18752).

230

Additional Information

232 Correspondence and requests for materials should be addressed to Barney S. Graham,

233 bgraham@nih.gov and Andrea Carfi, andrea.carfi@modernatx.com.

234

Methods

236 <u>MERS-CoV S-2P and SARS-CoV-2 S-2P mRNA synthesis and lipid nanoparticle formulation</u>

237 For each vaccine, T7 RNA polymerase-mediated transcription was used *in vitro* to synthesize

238 the mRNA from a linearized DNA template, which flanked the immunogen open-reading frames

239 with the 5′ and 3′ untranslated regions and a poly-A tail as described previously [29]. mRNA was

240 then purified, diluted in citrate buffer to the desired concentration and encapsulated into lipid

241 nanoparticles (LNP) by ethanol drop nanoprecipitation. At molar ratio of 50:10:38.5:1.5

242 (ionizable lipid:DSPC:cholesterol:PEG-lipid), lipids were dissolved in ethanol and combined with

243 a 6.25-mM sodium acetate buffer (pH 5) containing mRNA at a ratio of 3:1 (aqueous:ethanol).

244 Formulations were dialyzed against phosphate-buffered saline (pH 7.4) for at least 18 hr,

245 concentrated using Amicon ultracentrifugal filters (EMD Millipore), passed through a 0.22-μm

246 filter and stored at -20°C until use. All formulations underwent quality control for particle size,

247   RNA encapsulation, and endotoxin. LNP were between 80 – 100 nm in size, with > 90%

248   encapsulation on mRNA and < 10 EU/mL endotoxin.

249   <u>MERS-CoV and SARS-CoV Protein Expression and Purification</u>

250   Vectors encoding MERS-CoV S-2P[11] and SARS-CoV S-2P[22] were generated as previously

251   described with the following small amendments. Proteins were expressed by transfection of

252   plasmids into Expi293 cells using Expifectamine transfection reagent (ThermoFisher) in

253   suspension at 37°C for 4-5 days. Transfected cell culture supernatants were collected, buffer

254   exchanged into 1X PBS, and protein was purified using Strep-Tactin resin (IBA). For proteins

255   used for mouse inoculations, tags were cleaved with addition of HRV3C protease

256   (ThermoFisher) (1% wt/wt) overnight at 4 °C. Size exclusion chromatography using Superose 6

257   Increase column (GE Healthcare) yielded final purified protein.

258   <u>Design and Production of Recombinant Minifibritin Foldon Protein</u>

259   A mammalian codon-optimized plasmid encoding foldon inserted minifibritin

260   (ADIVLNDLPFVDGPPAEGQSRISWIKNGEEILGADTQYGSEGSMNRPTVSVLRNVEVLDKNIGI

261   LKTSLETANSDIKTIQEAGYIPEAPRDGQAYVRKDGEWVLLSTFLSPALVPRGSHHHHHHSAWS

262   HPQFEK) with a C-terminal thrombin cleavage site, 6x His-tag, and Strep-TagII was

263   synthesized and subcloned into a mammalian expression vector derived from pLEXm. The

264   construct was expressed by transient transfection of Expi293 (ThermoFisher) cells in

265   suspension at 37°C for 5 days. The protein was first purified with a Ni^{2+}-nitrilotriacetic acid (NTA)

266   resin (GE Healthcare,) using an elution buffer consisting of 50 mM Tris-HCl, pH 7.5, 400 mM

267   NaCl, and 300 mM imidazole, pH 8.0, followed by purification with StrepTactin resin (IBA)

268   according to the manufacturer's instructions.

269   <u>Cell Lines</u>

270   HEK293T/17 (ATCC #CRL-11268), Vero E6 (ATCC), Huh7.5 cells (provided by Deborah R.

271   Taylor, US Food and Drug Administration), and ACE-2-expressing 293T cells (provided by

272   Michael Farzan, Scripps Research Institute) were cultured in Dulbecco's modified Eagle's

273   medium (DMEM) supplemented with 10% FBS, 2 mM glutamine, and 1% penicillin/streptomycin

274   at 37°C and 5% CO_2. Vero E6 cells used in plaque assays to determine lung and nasal

275   turbinate viral titers were cultured in DMEM supplemented with 10% Fetal Clone II and 1%

276   anti/anti at 37C and 5% CO2. Vero E6 cells used in PRNT assays were cultured in DMEM

277   supplemented with 10% Fetal Clone II and amphotericin B [0.25 µg/ml] at 37C and 5% CO2.

278   Expi293 cells were maintained in manufacturer's suggested media.

279   *In vitro* mRNA Expression

280   HEK293T cells were transiently transfected with mRNA encoding SARS-CoV-2 WT S or S-2P

281   protein using a TranIT mRNA transfection kit (Mirus). After 24 hr, the cells were harvested and

282   resuspended in FACS buffer (1X PBS, 3% FBS, 0.05% sodium azide). To detect surface protein

283   expression, the cells were stained with 10 µg/mL ACE2-FLAG (Sigma) or CR3022[30] in FACS

284   buffer for 30 min on ice. Thereafter, cells were washed twice in FACS buffer and incubated with

285   FITC anti-FLAG (Sigma) or Alexafluor 647 goat anti-human IgG (Southern Biotech) in FACS

286   buffer for 30 min on ice. Live/Dead aqua fixable stain (Invitrogen) were utilized to assess

287   viability. Data acquisition was performed on a BD LSRII Fortessa instrument (BD Biosciences)

288   and analyzed by FlowJo software v10 (Tree Star, Inc.)

289   Mouse Models

290   Animal experiments were carried out in compliance with all pertinent US National Institutes of

291   Health regulations and approval from the Animal Care and Use Committee of the Vaccine

292   Research Center, Moderna Inc., or University of North Carolina at Chapel Hill. For

293   immunogenicity studies, 6-8-week-old female BALB/c (Charles River), BALB/cJ, C57BL/6J, or

294   B6C3F1/J mice (Jackson Laboratory) were used. mRNA formulations were diluted in 50 µL of

295   1X PBS, and mice were inoculated IM into the same hind leg for both prime and boost. For all

296   SARS-CoV-2 S-P protein vaccinations, mice were inoculated IM, with SAS, as previously

297   detailed[11]. For S + alum immunizations, SARS-CoV-2 S protein (Sino Biological) + 250 μg alum

298   hydrogel was delivered IM. For challenge studies to evaluate MERS-CoV-2 vaccines, 16-20-

299   week-old 288/330$^{+/+}$mice[21] were immunized. Four weeks post-boost, pre-challenge sera were

300   collected from a subset of mice, and remaining mice were challenged with 5x10^5 PFU of a

301   mouse-adapted MERS-CoV EMC derivative, m35c4[31]. On day 3 post-challenge, lungs were

302   harvested, and hemorrhage and viral titer were assessed, per previously published methods[32].

303   For challenge studies to evaluate SARS-CoV-2 vaccines, BALB/cJ mice were challenged with

304   10^5 PFU of mouse-adapted SARS-CoV-2 (SARS-CoV-2 MA). On day 2 post-challenge, lungs

305   and nasal turbinates were harvested for viral titer assessment, per previously published

306   methods[28].

307   Histology

308   Lungs from mice were collected at the indicated study endpoints and placed in 10% neutral

309   buffered formalin (NBF) until adequately fixed. Thereafter, tissues were trimmed to a thickness

310   of 3-5 mm, processed and paraffin embedded. The respective paraffin tissue blocks

311   were sectioned at 5 μm and stained with hematoxylin and eosin (H&E). All sections were

312   examined by a board-certified veterinary pathologist using an Olympus BX51 light microscope

313   and photomicrographs were taken using an Olympus DP73 camera.

314   Enzyme-linked Immunosorbent Assay (ELISA)

315   Nunc Maxisorp ELISA plates (ThermoFisher) were coated with 100 ng/well of protein in 1X PBS

316   at 4°C for 16 hr. Where applicable, to eliminate fold-on-specific binding from MERS S-2P- or

317   SARS-CoV-2 S-2P protein-immune mouse serum, 50 µg/mL of fold-on protein was added for 1

318   hr at room temperature (RT). After standard washes and blocks, plates were incubated with

319   serial dilutions of heat-inactivated (HI) sera for 1 hr at RT. Following washes, anti-mouse IgG,

320   IgG1, or IgG2a or IgG2c–horseradish peroxidase conjugates (ThermoFisher) were used as

321   secondary Abs, and 3,5,3′5′-tetramethylbenzidine (TMB) (KPL) was used as the substrate to

322   detect Ab responses. Endpoint titers were calculated as the dilution that emitted an optical

323   density exceeding 4X background (secondary Ab alone).

324   Pseudovirus Neutralization Assay

325   We introduced divergent amino acids, as predicted from translated sequences, into the CMV/R-

326   MERS-CoV EMC S (GenBank#: AFS88936) gene[33] to generate a MERS-CoV m35c4 S gene[31].

327   To produce SARS-CoV-2 pseudoviruses, a codon-optimized CMV/R-SARS-CoV-2 S (Wuhan-1,

328   Genbank #: MN908947.3) plasmid was constructed. Pseudoviruses were produced by co-

329   transfection of plasmids encoding a luciferase reporter, lentivirus backbone, and S genes into

330   HEK293T/17 cells (ATCC #CRL-11268), as previously described[33]. For SARS-CoV-2

331   pseudovirus, human transmembrane protease serine 2 (TMPRSS2) plasmid was also co-

332   transfected[34]. Pseudoneutralization assay methods have been previously described[11]. Briefly, HI

333   serum was mixed with pseudoviruses, incubated, and then added to Huh7.5 cells or ACE-2-

334   expressing 293T cells, for MERS-CoV and SARS-CoV-2 respectively. Seventy-two hr later, cells

335   were lysed, and luciferase activity (relative light units, RLU) was measured. Percent

336   neutralization was normalized considering uninfected cells as 100% neutralization and cells

337   infected with only pseudovirus as 0% neutralization. IC_{50} titers were determined using a log

338   (agonist) vs. normalized response (variable slope) nonlinear function in Prism v8 (GraphPad).

339   Plaque Reduction Neutralization Test (PRNT)

340   HI sera were diluted in gelatin saline (0.3% [wt/vol] gelatin in phosphate-buffered saline

341   supplemented with $CaCl_2$ and $MgCl_2$) to generate a 1:5 dilution of the original specimen, which

342   served as a starting concentration for further serial log_4 dilutions terminating in 1:81,920. Sera

343   were combined with an equal volume of SARS-CoV-2 clinical isolate 2019-nCoV/USA-WA1-

344   F6/2020 in gelatin saline, resulting in an average concentration of 730 plaque-forming units per

345   mL (determined from plaque counts of 24 individual wells of untreated virus) in each serum

346   dilution. Thus, final serum concentrations ranged from 1:10 to 1:163,840 of the original.

347   Virus/serum mixtures were incubated for 20 min at 37 $^\circ$C, followed by adsorption of 0.1 mL to

348   each of two confluent Vero E6 cell monolayers (in 10-cm^2 wells) for 30 min at 37°C. Cell

349   monolayers were overlaid with Dulbecco's modified Eagle's medium (DMEM) containing 1%

350   agar and incubated for 3 d at 37°C in humidified 5% CO_2. Plaques were enumerated by direct

351   visualization. The average number of plaques in virus/serum (duplicate) and virus-only (24)

352   wells was used to generate percent neutralization curves according the following formula: 1 –

353   (ratio of mean number of plaques in the presence and absence of serum). The PRNT IC_{50} titer

354   was defined as the reciprocal serum dilution at which the neutralization curve crossed the 50%

355   threshold.

356   Intracellular Cytokine Staining

357   Mononuclear single cell suspensions from whole mouse spleens were generated using a

358   gentleMACS tissue dissociator (Miltenyi Biotec) followed by 70 µm filtration and density gradient

359   centrifugation using Fico/Lite-LM medium (Atlanta Biologicals). Cells from each mouse were

360   resuspended in R10 media (RPMI 1640 supplemented with Pen-Strep antibiotic, 10% HI-FBS,

361   Glutamax, and HEPES) and incubated for 6 hr at 37°C with protein transport inhibitor cocktail

362   (eBioscience) under three conditions: no peptide stimulation, and stimulation with two spike

363   peptide pools (JPT product PM-WCPV-S-1). Peptide pools were used at a final concentration of

364   2 µg/mL each peptide. Cells from each group were pooled for stimulation with cell stimulation

365   cocktail (eBioscience) as a positive control. Following stimulation, cells were washed with PBS

366   prior to staining with LIVE/DEAD Fixable Blue Dead Cell Stain (Invitrogen) for 20 min at RT.

367   Cells were then washed in FC buffer (PBS supplemented with 2% HI-FBS and 0.05% NaN_3)

368   and resuspended in BD Fc Block (clone 2.4G2) for 5 min at RT prior to staining with a surface

369   stain cocktail containing the following antibodies purchased from BD and Biolegend: I-A/I-E

370   (M5/114.15.2) PE, CD8a (53-6.7) BUV805, CD44 (IM7) BUV395, CD62L (MEL-14) BV605, and

371   CD4 (RM4-5) BV480 in brilliant stain buffer (BD). After 15 min, cells were washed with FC buffer

372   then fixed and permeabilized using the BD Cytofix/Cytoperm fixation/permeabilization solution

373   kit according to manufacturer instructions. Cells were washed in perm/wash solution and

374   stained with Fc Block (5 min at RT), followed by intracellular staining (30 min at 4°C) using a

375   cocktail of the following antibodies purchased from BD, Biolegend, or eBioscience: CD3e (17A2)

376   BUV737, IFN-γ (XMG1.2) BV650, TNF-α (MP6-XT22) BV711, IL-2 (JES6-5H4) BV421, IL-4

377   (11B11) Alexa Fluor 488, and IL-5 (TRFK5) APC in 1x perm/wash diluted with brilliant stain

378   buffer. Finally, cells were washed in perm/wash solution and resuspended in 0.5% PFA-FC

379   stain buffer prior to running on a Symphony A5 flow cytometer (BD). Analysis was performed

380   using FlowJo software, version 10.6.2 according to the gating strategy outlined in **Extended**

381   **Data Figure 9.** Background cytokine expression in the no peptide condition was subtracted from

382   that measured in the S1 and S2 peptide pools for each individual mouse.

383   T Cell Stimulation and Cytokine Analysis

384   Spleens from immunized mice were collected 2 weeks post-boost. 2×10^6 splenocytes/well (96-

385   well plate) were stimulated *in vitro* with two peptide libraries, JPT1 and JPT2, (15mers with 11

386   aa overlap) covering the entire SARS-CoV-2 spike protein (JPT product PM-WCPV-S-1). Both

387   peptide libraries were used at a final concentration of 1 µg/mL. After 24 hr of culture at 37°C, the

388   plates were centrifuged and supernatant was collected and frozen at -80°C for cytokine

389   detection. Measurements and analyses of secreted cytokines from a murine 35-plex kit were

390   performed using a multiplex bead-based technology (Luminex) assay with a Bio-Plex 200

391   instrument (Bio-Rad) after 2-fold dilution of supernatants.

392   <u>Statistical Analysis</u>

393   Geometric means or means are represented by the heights of bars, or symbols, and error bars

394   represent the corresponding SD. Dotted lines indicate assay limits of detection. Mann-Whitney

395   tests were used to compare 2 experimental groups and Wilcoxon signed rank tests to compare

396   the same animals at different time points. To compare >2 experimental groups, Kruskal-Wallis

397   ANOVA with Dunn's multiple comparisons tests were applied. For antibody responses

398   in **Extended Data Fig. 4c**, a Spearman correlation test was used to correlate binding antibody

399   titers to neutralizing antibody titers. * = p-value < 0.05, ** = p-value < 0.01, *** = p-value < 0.001,

400   **** = p-value < 0.0001.

References

401

402

403   1   Dong, E., Du, H. & Gardner, L. An interactive web-based dashboard to track COVID-19
404   in real time. *The Lancet Infectious Diseases* **20**, 533-534,
405   doi:https://doi.org/10.1016/S1473-3099(20)30120-1 (2020).
406   2   Keni, R., Alexander, A., Nayak, P. G., Mudgal, J. & Nandakumar, K. COVID-19:
407   Emergence, Spread, Possible Treatments, and Global Burden. *Frontiers in Public Health*
408   **8**, doi:10.3389/fpubh.2020.00216 (2020).
409   3   Graham, B. S. Rapid COVID-19 vaccine development. *Science* **368**, 945-946,
410   doi:10.1126/science.abb8923 (2020).
411   4   Graham, B. S., Gilman, M. S. A. & McLellan, J. S. Structure-Based Vaccine Antigen
412   Design. *Annu Rev Med* **70**, 91-104, doi:10.1146/annurev-med-121217-094234 (2019).
413   5   McLellan, J. S. *et al.* Structure of RSV fusion glycoprotein trimer bound to a prefusion-
414   specific neutralizing antibody. *Science* **340**, 1113-1117, doi:10.1126/science.1234914
415   (2013).
416   6   McLellan, J. S. *et al.* Structure-based design of a fusion glycoprotein vaccine for
417   respiratory syncytial virus. *Science* **342**, 592-598, doi:10.1126/science.1243283 (2013).
418   7   Crank, M. C. *et al.* A proof of concept for structure-based vaccine design targeting RSV
419   in humans. *Science* **365**, 505-509 (2019).
420   8   Gilman, M. S. A. *et al.* Rapid profiling of RSV antibody repertoires from the memory B
421   cells of naturally infected adult donors. *Sci Immunol* **1**, doi:10.1126/sciimmunol.aaj1879
422   (2016).
423   9   Walls, A. C. *et al.* Cryo-electron microscopy structure of a coronavirus spike glycoprotein
424   trimer. *Nature* **531**, 114-117, doi:10.1038/nature16988 (2016).
425   10   Kirchdoerfer, R. N. *et al.* Pre-fusion structure of a human coronavirus spike protein.
426   *Nature* **531**, 118-121, doi:10.1038/nature17200 (2016).
427   11   Pallesen, J. *et al.* Immunogenicity and structures of a rationally designed prefusion
428   MERS-CoV spike antigen. *Proceedings of the National Academy of Sciences* **114**,
429   E7348-E7357, doi:10.1073/pnas.1707304114 (2017).
430   12   Graham, B. S. & Sullivan, N. J. Emerging viral diseases from a vaccinology perspective:
431   preparing for the next pandemic. *Nat Immunol* **19**, 20-28, doi:10.1038/s41590-017-0007-
432   9 (2018).
433   13   Graham, B. S. & Corbett, K. S. Prototype pathogen approach for pandemic
434   preparedness: world on fire. *J Clin Invest*, doi:10.1172/JCI139601 (2020).
435   14   Menachery, V. D. *et al.* A SARS-like cluster of circulating bat coronaviruses shows
436   potential for human emergence. *Nat Med* **21**, 1508-1513, doi:10.1038/nm.3985 (2015).
437   15   Menachery, V. D. *et al.* SARS-like WIV1-CoV poised for human emergence. *Proc Natl
438   Acad Sci U S A* **113**, 3048-3053, doi:10.1073/pnas.1517719113 (2016).
439   16   Graham, B. S., Mascola, J. R. & Fauci, A. S. Novel Vaccine Technologies: Essential
440   Components of an Adequate Response to Emerging Viral Diseases. *JAMA* **319**, 1431-
441   1432, doi:10.1001/jama.2018.0345 (2018).
442   17   Dowd, K. A. *et al.* Rapid development of a DNA vaccine for Zika virus. *Science* **354**, 237-
443   240 (2016).
444   18   Pardi, N., Hogan, M. J., Porter, F. W. & Weissman, D. mRNA vaccines - a new era in
445   vaccinology. *Nat Rev Drug Discov* **17**, 261-279, doi:10.1038/nrd.2017.243 (2018).
446   19   Hassett, K. J. *et al.* Optimization of Lipid Nanoparticles for Intramuscular Administration
447   of mRNA Vaccines. *Mol Ther Nucleic Acids* **15**, 1-11, doi:10.1016/j.omtn.2019.01.013
448   (2019).
449   20   Mauger, D. M. *et al.* mRNA structure regulates protein expression through changes in
450   functional half-life. *Proceedings of the National Academy of Sciences* **116**, 24075,
451   doi:10.1073/pnas.1908052116 (2019).

21   Cockrell, A. S. *et al.* A mouse model for MERS coronavirus-induced acute respiratory distress syndrome. *Nat Microbiol* **2**, 16226-16226, doi:10.1038/nmicrobiol.2016.226 (2016).

22   Wrapp, D. *et al.* Cryo-EM structure of the 2019-nCoV spike in the prefusion conformation. *Science* **367**, 1260-1263, doi:10.1126/science.abb2507 (2020).

23   Freeman, B. *et al.* Validation of a SARS-CoV-2 spike protein ELISA for use in contact investigations and sero-surveillance. *bioRxiv* (2020).

24   Klumpp-Thomas, C. *et al.* Standardization of enzyme-linked immunosorbent assays for serosurveys of the SARS-CoV-2 pandemic using clinical and at-home blood sampling. *medRxiv*, 2020.2005.2021.20109280, doi:10.1101/2020.05.21.20109280 (2020).

25   Kim, H. W. *et al.* RESPIRATORY SYNCYTIAL VIRUS DISEASE IN INFANTS DESPITE PRIOR ADMINISTRATION OF ANTIGENIC INACTIVATED VACCINE12. *American Journal of Epidemiology* **89**, 422-434, doi:10.1093/oxfordjournals.aje.a120955 (1969).

26   Fulginiti, V. A., Eller, J. J., Downie, A. W. & Kempe, C. H. Altered Reactivity to Measles Virus: Atypical Measles in Children Previously Immunized With Inactivated Measles Virus Vaccines. *JAMA* **202**, 1075-1080, doi:10.1001/jama.1967.03130250057008 (1967).

27   Bolles, M. *et al.* A Double-Inactivated Severe Acute Respiratory Syndrome Coronavirus Vaccine Provides Incomplete Protection in Mice and Induces Increased Eosinophilic Proinflammatory Pulmonary Response upon Challenge. *Journal of Virology* **85**, 12201, doi:10.1128/JVI.06048-11 (2011).

28   Dinnon, K. H. *et al.* A mouse-adapted SARS-CoV-2 model for the evaluation of COVID-19 medical countermeasures. *bioRxiv,* 2020.2005.2006.081497, doi:10.1101/2020.05.06.081497 (2020).

29   Richner, J. M. *et al.* Modified mRNA Vaccines Protect against Zika Virus Infection. *Cell* **169**, 176, doi:10.1016/j.cell.2017.03.016 (2017).

30   ter Meulen, J. *et al.* Human Monoclonal Antibody Combination against SARS Coronavirus: Synergy and Coverage of Escape Mutants. *PLOS Medicine* **3**, e237, doi:10.1371/journal.pmed.0030237 (2006).

31   Douglas, M. G., Kocher, J. F., Scobey, T., Baric, R. S. & Cockrell, A. S. Adaptive evolution influences the infectious dose of MERS-CoV necessary to achieve severe respiratory disease. *Virology* **517**, 98-107, doi:10.1016/j.virol.2017.12.006 (2018).

32   Scobey, T. *et al.* Reverse genetics with a full-length infectious cDNA of the Middle East respiratory syndrome coronavirus. *Proceedings of the National Academy of Sciences* **110**, 16157, doi:10.1073/pnas.1311542110 (2013).

33   Wang, L. *et al.* Evaluation of candidate vaccine approaches for MERS-CoV. *Nature Communications* **6**, 7712, doi:10.1038/ncomms8712 (2015).

34   Bottcher, E. *et al.* Proteolytic activation of influenza viruses by serine proteases TMPRSS2 and HAT from human airway epithelium. *J Virol* **80**, 9896-9898, doi:10.1128/JVI.01118-06 (2006).
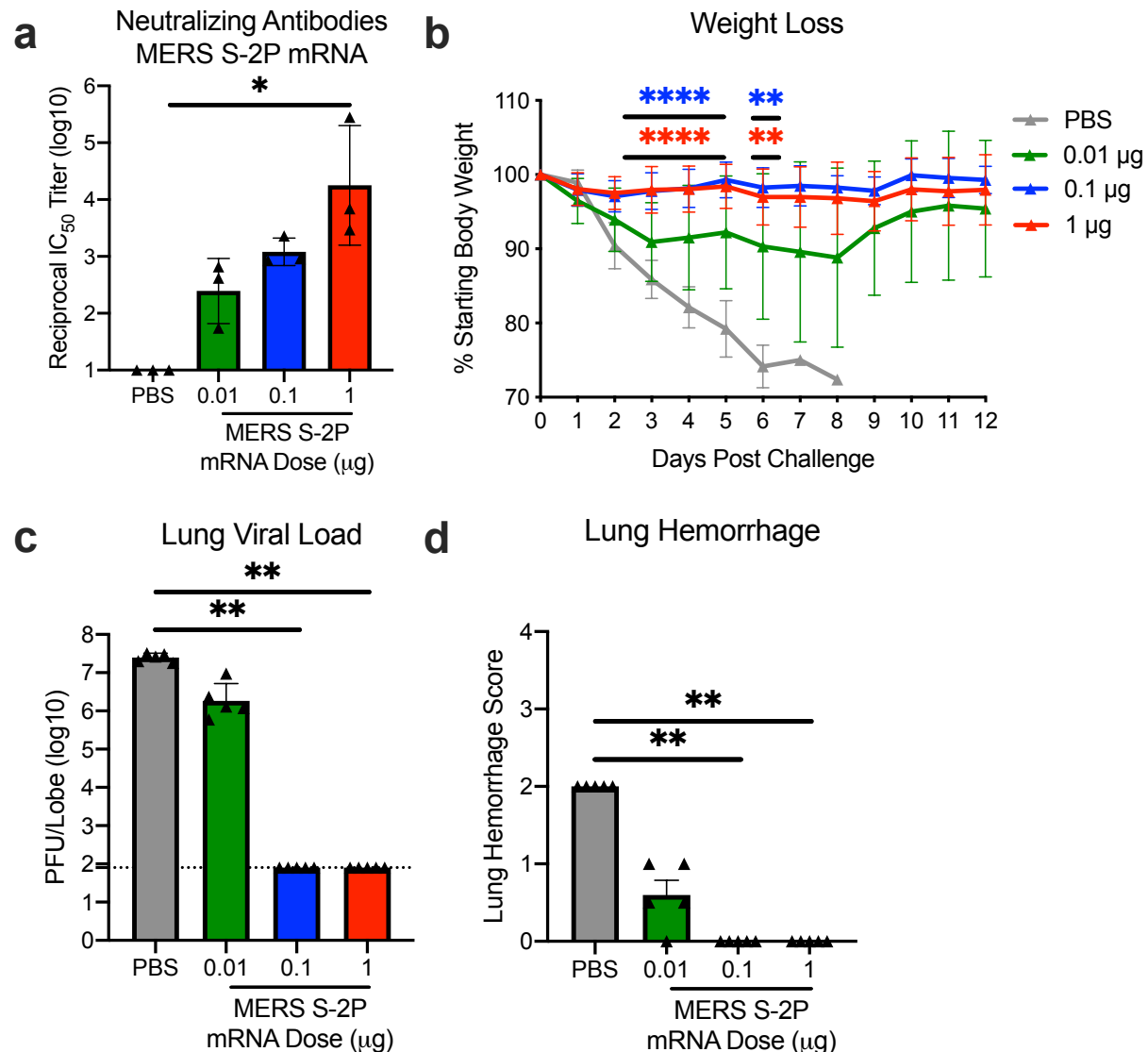
Figure 1

Figure 1. **MERS-CoV S-2P mRNA protects mice from lethal challenge.** 288/330[+/+] mice were immunized at weeks 0 and 3 with 0.01 (green), 0.1 (blue), or 1 µg (red) of MERS-CoV S-2P mRNA. Mock-immunized mice were immunized with PBS (gray). Two weeks post-boost, sera were collected from 3 mice per group and assessed for neutralizing antibodies against MERS m35c4 pseudovirus (a). Four weeks post-boost, 12 mice per group were challenged with a lethal dose of mouse-adapted MERS-CoV (m35c4). Following challenge, mice were monitored for weight loss (b). Two days post-challenge, at peak viral load, lung viral titers (c) and hemorrhage (0 = no hemorrhage, 4 = severe hemorrhage in all lobes) (d) were assessed from 5 animals per

Figure 1

503   group. Dotted line = assay limit of detection. (a, c-d) All dose levels were compared. (b) For

504   weight loss, all comparisons are against PBS-immunized mice.

Figure 1
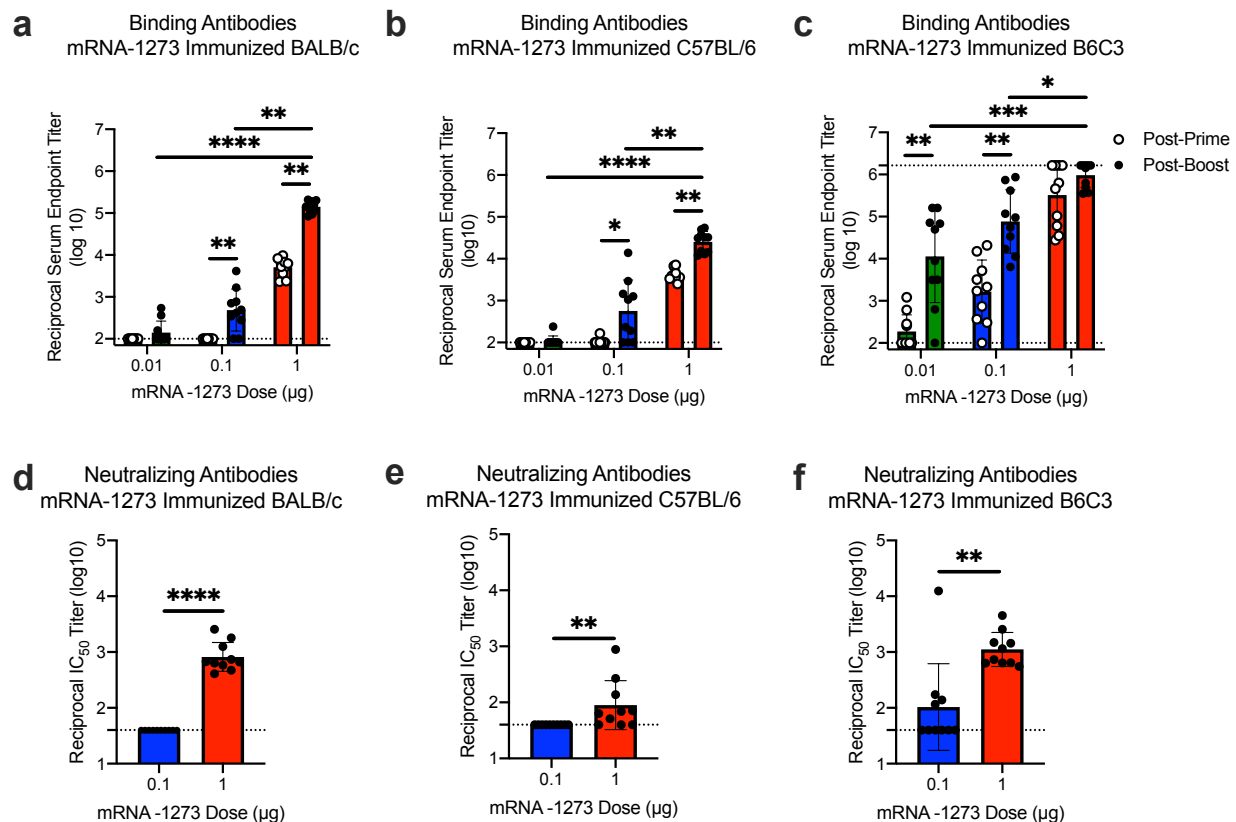
Figure 2

Figure 2. mRNA-1273 elicits robust binding and neutralizing antibody responses in multiple mouse strains. BALB/cJ (a, d), C57BL/6J (b, e), or B6C3F1/J (c, f) mice were immunized at weeks 0 and 3 weeks with 0.01 (green), 0.1 (blue), or 1 µg (red) of mRNA-1273. Sera were collected 2 weeks post-prime (open circles) and 2 weeks post-boost (closed circles) and assessed for SARS-CoV-2 S-specific IgG by ELISA (a-c), and, for post-boost sera, neutralizing antibodies against homotypic SARS-CoV-2 pseudovirus (d-f). Dotted line = assay limit of detection. (a-c) Timepoints were compared within each dose level, and doses were compared post-boost.

Figure 3
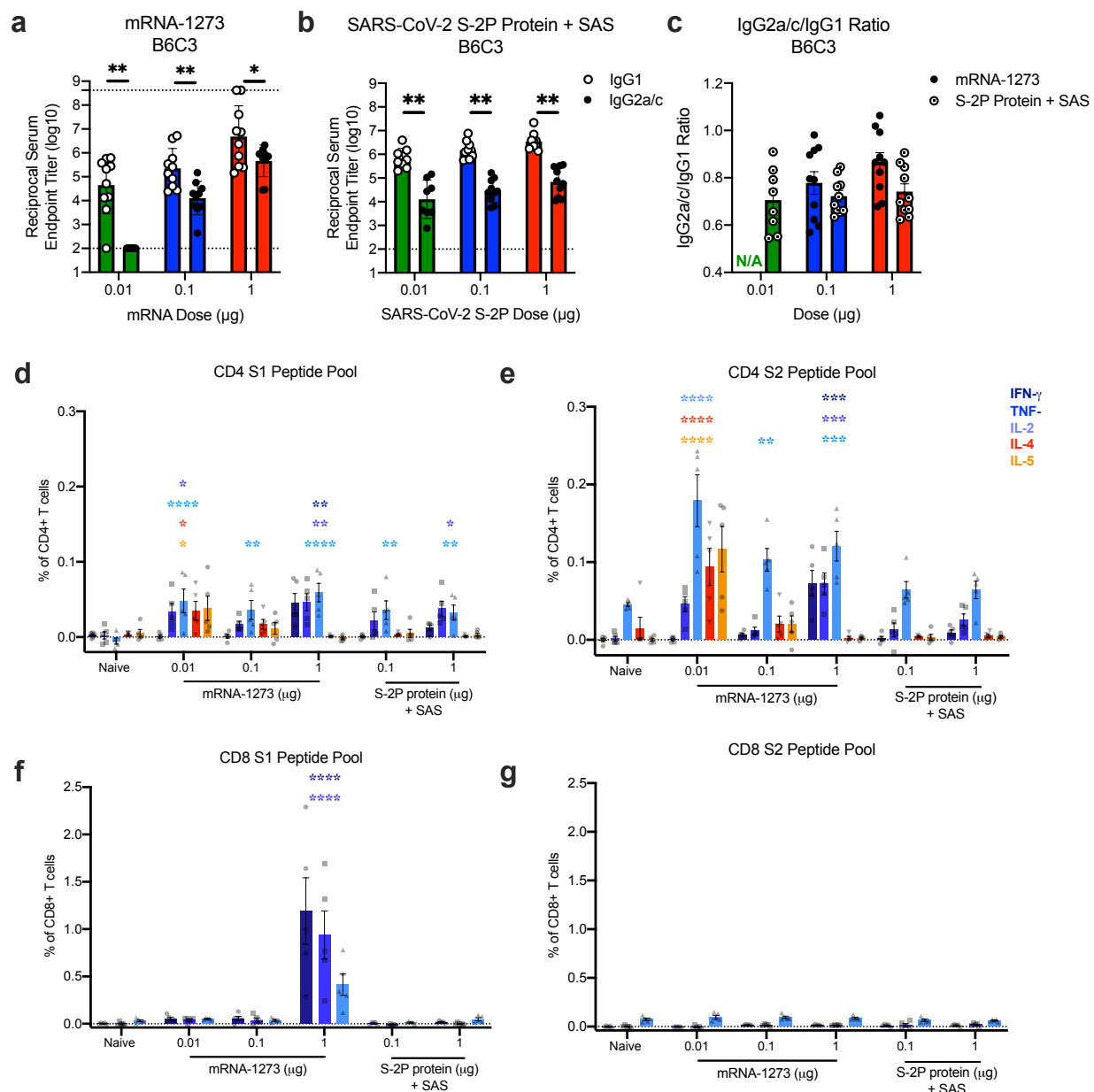
Figure 3. Immunizations with mRNA-1273 and S-2P protein, delivered with TLR4 agonist, elicit S-specific Th1-biased T cell responses. B6C3F1/J mice were immunized at weeks 0 and 3 with 0.01, 0.1, or 1 µg of mRNA-1273 or SAS-adjuvanted SARS-CoV-2 S-2P protein. Sera were collected 2 weeks post-boost and assessed by ELISA for SARS-CoV-2 S-specific IgG1 and IgG2a/c. Endpoint titers (a-b) and endpoint titer ratios of IgG2a/c to IgG1 (c) were calculated. For mice for which endpoint titers did not reach the lower limit of detection (dotted line), ratios were

Figure 3

not calculated (N/A). (d-g) Seven weeks post-boost, splenocytes were isolated from 5 mice per group and re-stimulated with no peptides or pools of overlapping peptides from SARS-CoV-2 S protein in the presence of a protein transport inhibitor cocktail. After 6 hours, intracellular cytokine staining (ICS) was performed to quantify CD4+ and CD8+ T cell responses. Cytokine expression in the presence of no peptides was considered background and subtracted from the responses measured from the S1 and S2 peptide pools for each individual mouse. (d-e) CD4+ T cells expressing IFN-γ, TNFα, IL-2, IL-4 and IL-5 in response to the S1 (d) and S2 (e) peptide pools. (f-g) CD8+ T cells expressing IFN-γ, TNF-α, and IL-2 in response to the S1 (f) and S2 (g) peptide pools. IgG1 and IgG2a/c (a-b) and immunogens (c) were compared at each dose level. (d-g) For each cytokine, all comparisons were compared to naïve mice.

Figure 4
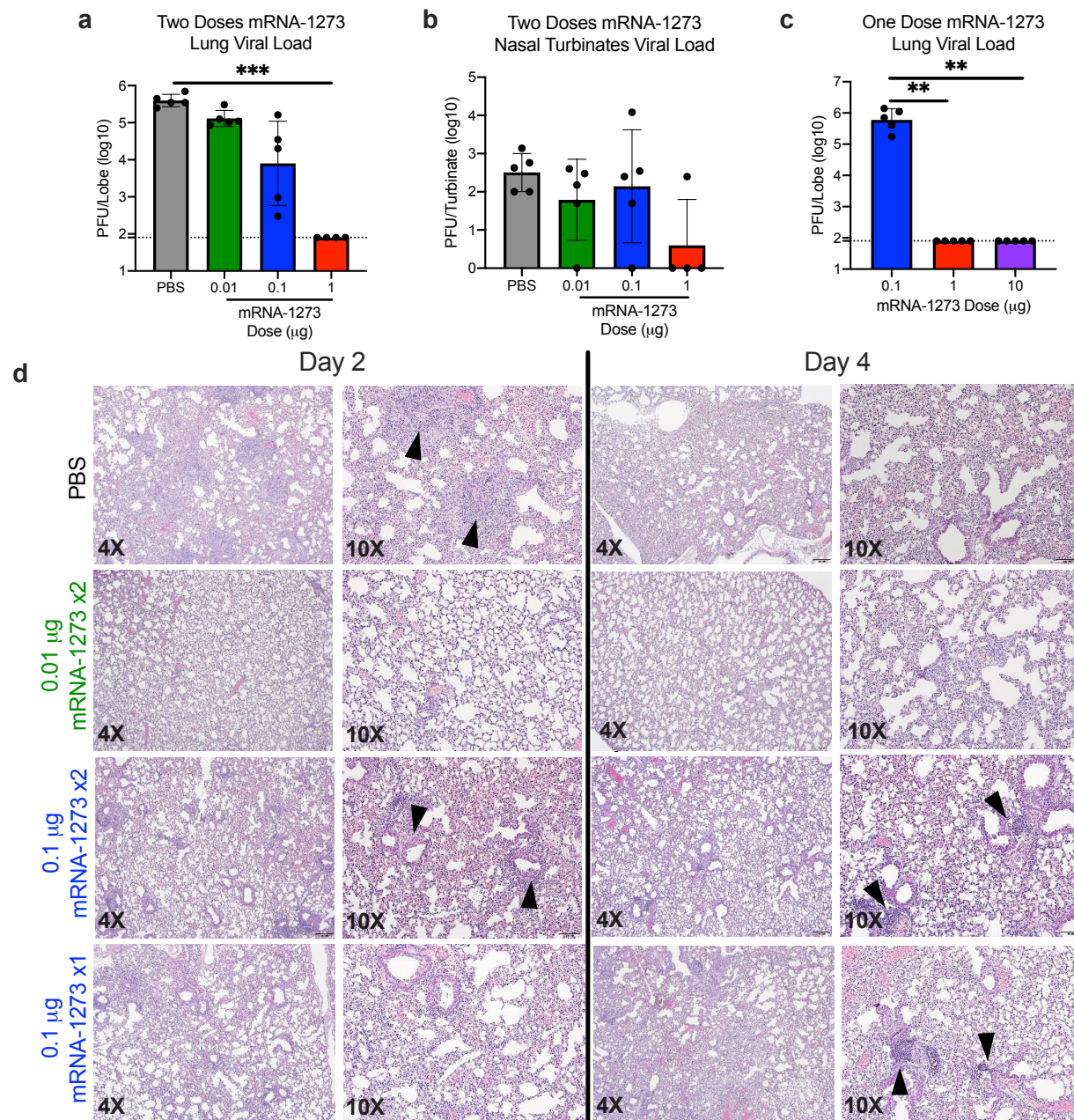
Figure 4. mRNA-1273 protects mice from upper and lower airway SARS-CoV-2 infection.

(a-b) BALB/cJ mice were immunized at weeks 0 and 3 with 0.01 (green), 0.1 (blue), or 1 µg (red) of mRNA-1273. Mock-immunized mice were immunized with PBS x2. Five weeks post-boost, mice were challenged with mouse-adapted SARS-CoV-2. (c) BALB/cJ mice were also immunized with a single dose of 0.1 (blue),1 (red), or 10 (purple) µg of mRNA-1273 and challenged 7 weeks post-immunization. Two days post-challenge, at peak viral load, mouse lungs (a,c) and nasal

Figure 4

turbinates (b) were harvested from 5 mice group for analysis of viral titers. Dotted line = assay limit of detection. (d) At day 2 and 4 post-challenge, lungs from 5 mice per group were fixed in 10% formalin, paraffin-embedded, cut in 5 μm sections, and stained with hematoxylin and eosin. Photomicrographs (4X and 10X) are representative of lung sections from groups of mice in which virus infection was detected. At day 2, lungs from mock-immunized mice demonstrated moderate to severe, predominantly neutrophilic, inflammation that was present within, and surrounding, small bronchioles (arrowheads); the surrounding alveolar capillaries were markedly expanded by infiltrating inflammatory cells. In the 0.01 μg two-dose group, inflammation was minimal to absent. In the 0.1 μg two-dose group, occasional areas of inflammation intimately associated with small airways (bronchioles) and their adjacent vasculature (arrowheads) were seen, primarily composed of neutrophils. In the single-dose 0.1 μg group, there were mild patchy expansion of the alveolar septae by mononuclear and polymorphonuclear cells. At day 4, lungs from mock-immunized mice exhibited moderate to marked expansion of the alveolar septae (interstitial pattern) with decreased prominence of the adjacent alveolar spaces. In the 0.01 μg two-dose group, inflammation was minimal to absent. Lungs in the 0.1 μg two-dose group showed mild, predominantly lymphocytic inflammation, intimately associated with bronchioles and adjacent vasculature (arrowheads). In the single-dose 0.1 μg group there was mild, predominantly lymphocytic, inflammation around bronchovascular bundles (arrowheads).
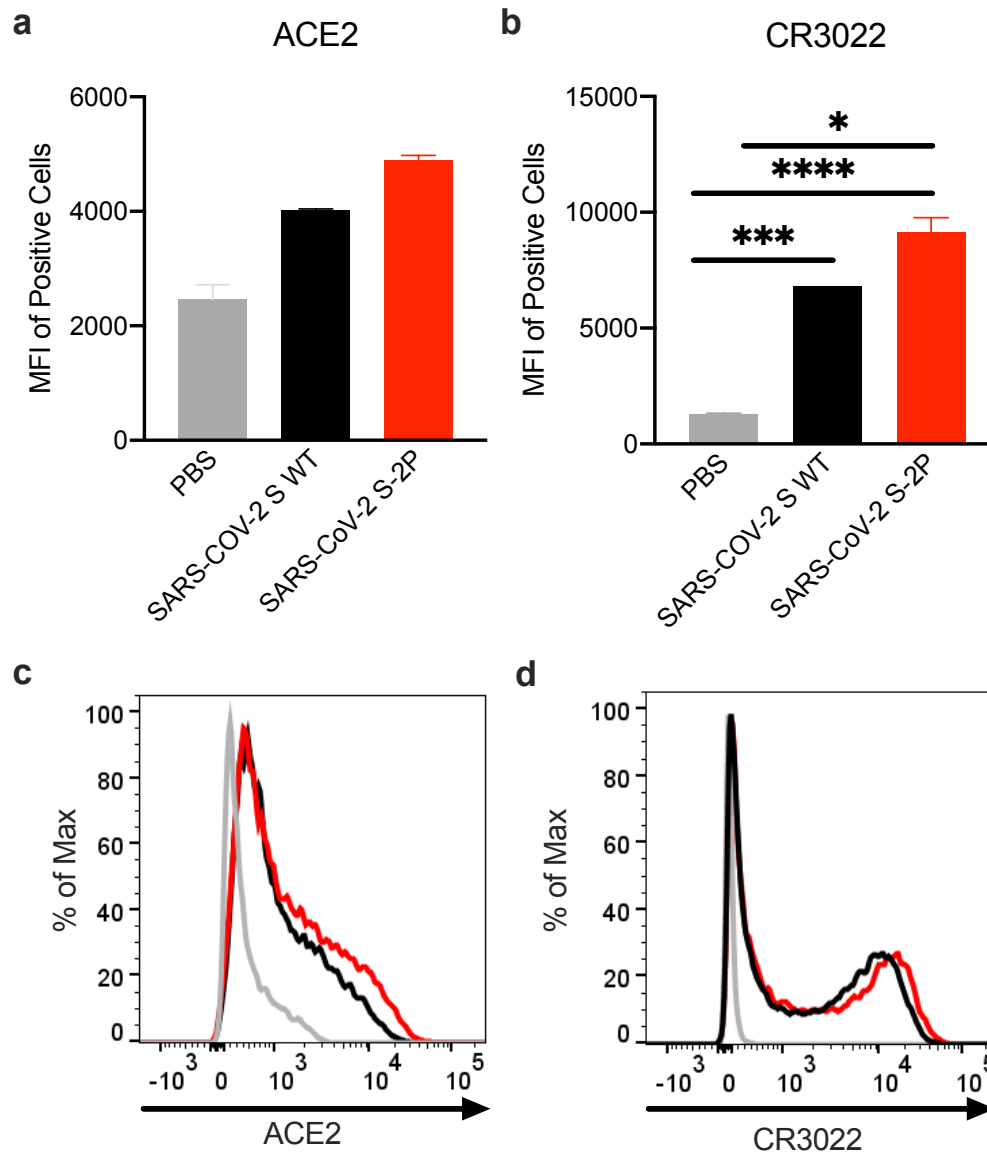
Extended Data Figure 1. **Transmembrane-anchored MERS-CoV S-2P (S-2P_TM) mRNA elicits more potent neutralizing antibody responses than secreted MERS-CoV S-2P and S WT mRNA.** C57BL/6J mice were immunized at weeks 0 and 4 with (a) 0.4, 2, or 10 µg of MERS-CoV S-2P_TM (red) or MERS S-2P_secreted (red hashed) or (b) 0.016 µg, 0.08 µg, or 0.4 µg of MERS-CoV S-2P or MERS-CoV S WT_TM (black) mRNA. Sera were collected 4 weeks post-boost and assessed for neutralizing antibodies against MERS-CoV m35c4 pseudovirus. Dotted line = assay limit of detection. Immunogens were compared at each dose level
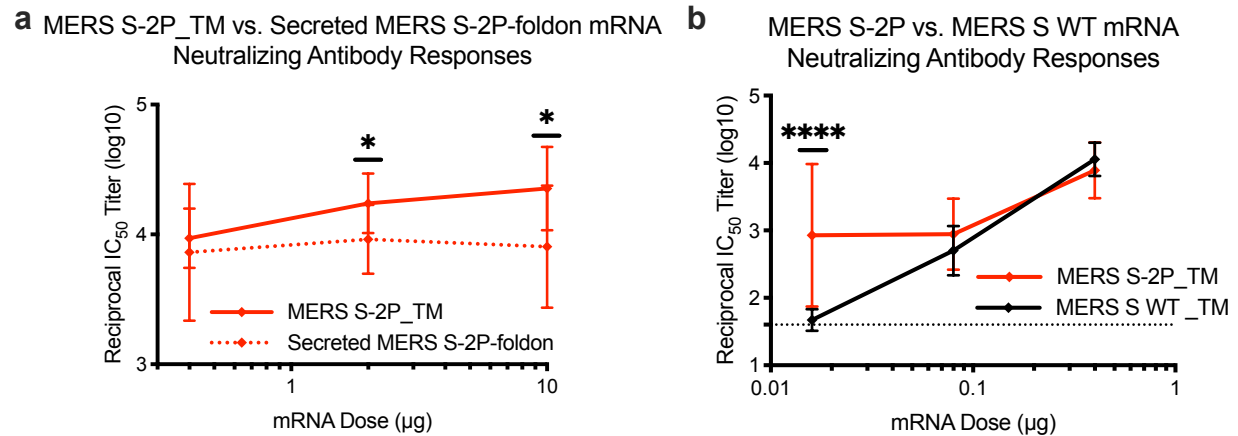
Extended Data Figure 2. **Timeline for mRNA-1273's progression to clinical trial.** The morning after novel coronavirus (nCoV) sequences were released, spike sequences were modified to include prefusion stabilizing mutations and synthesized for protein production, assay development, and vaccine development. Twenty-five days after viral sequences were released, clinically-relevant mRNA-1273 was received to initiate animal experiments. Immunogenicity in mice was confirmed 15 days later. Moderna shipped clinical drug product 41 days after GMP production began, leading to the Phase 1 clinical trial starting 66 days following the release of nCoV sequences.
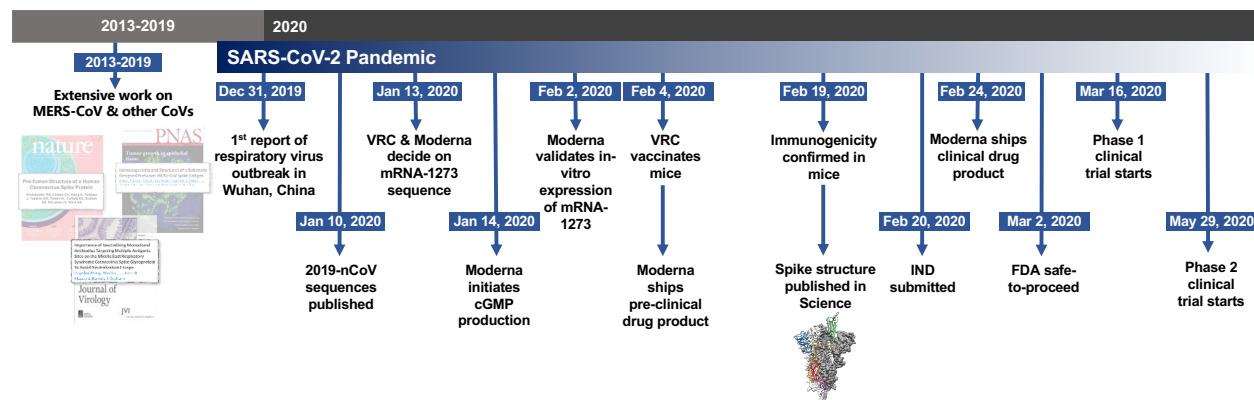
Extended Data Figure 3. *In vitro* **expression of SARS-CoV-2 spike mRNA on cell surface.**

293T cells were transfected with mRNA expressing SARS-CoV-2 wild-type spike (black) or S-2P (red), stained with ACE2 (a,c) or CR3022 (b,d), and evaluated by flow cytometry 24 post-transfection. Mock-transfected (PBS) cells served as a control.

Extended Data Figure 4. **Dose-dependent mRNA-1273-elicited antibody responses reveal strong positive correlation between binding and neutralization titers.** BALB/cJ mice were immunized at weeks 0 and 3 weeks with various doses (0.0025 – 20 µg) of mRNA-1273. (a-b) Sera were collected 2 weeks post-boost and assessed for SARS-CoV-2 S-specific IgG by ELISA (a) and neutralizing antibodies against homotypic SARS-CoV-2 pseudovirus (b). (a-b) All doses were compared to 20 µg dose.
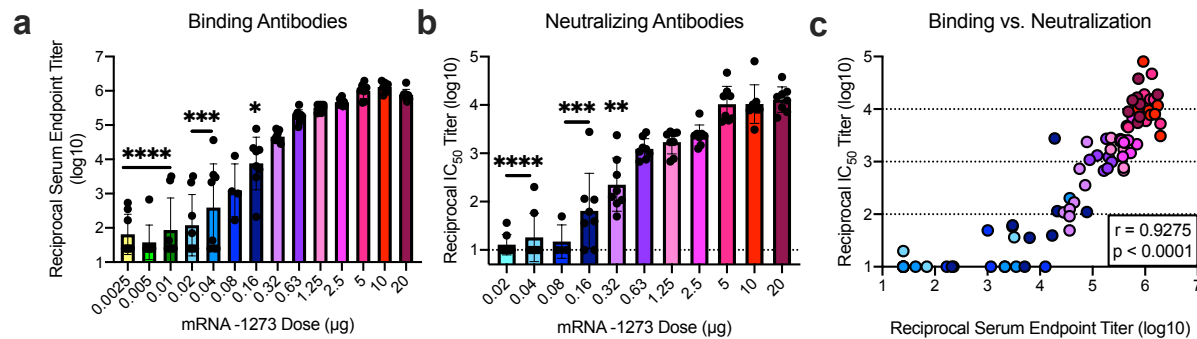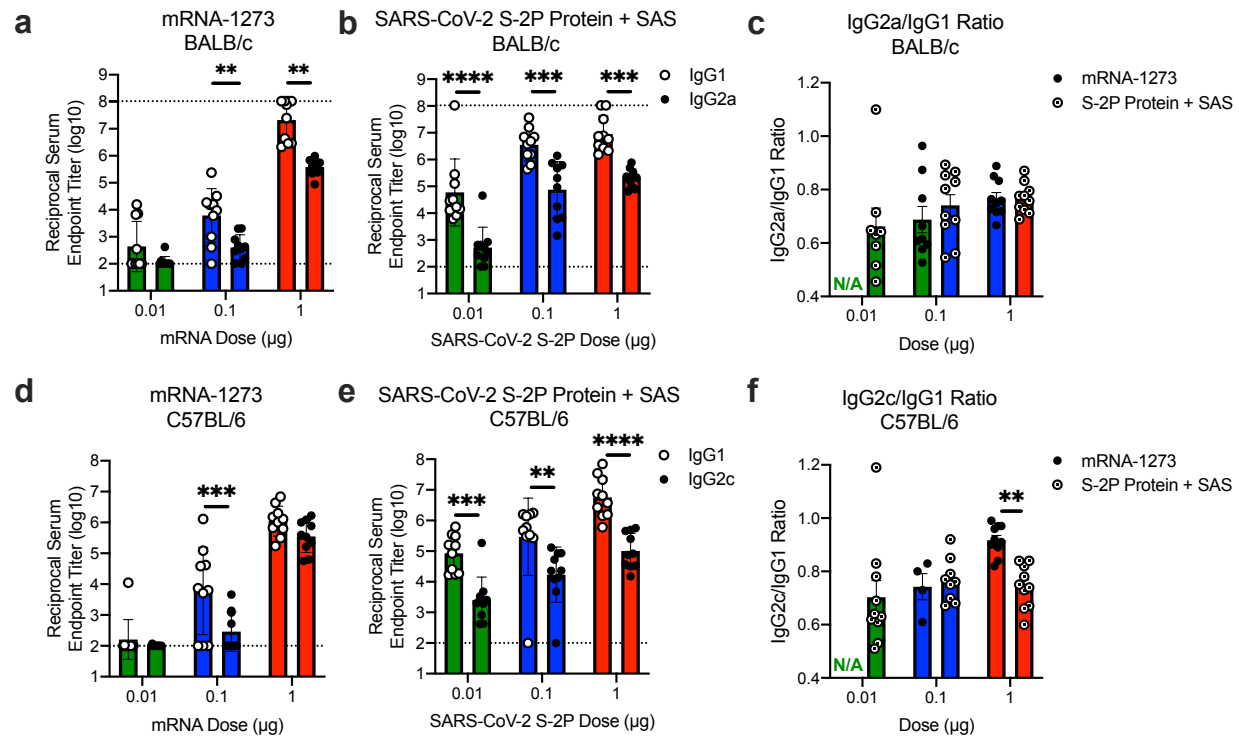
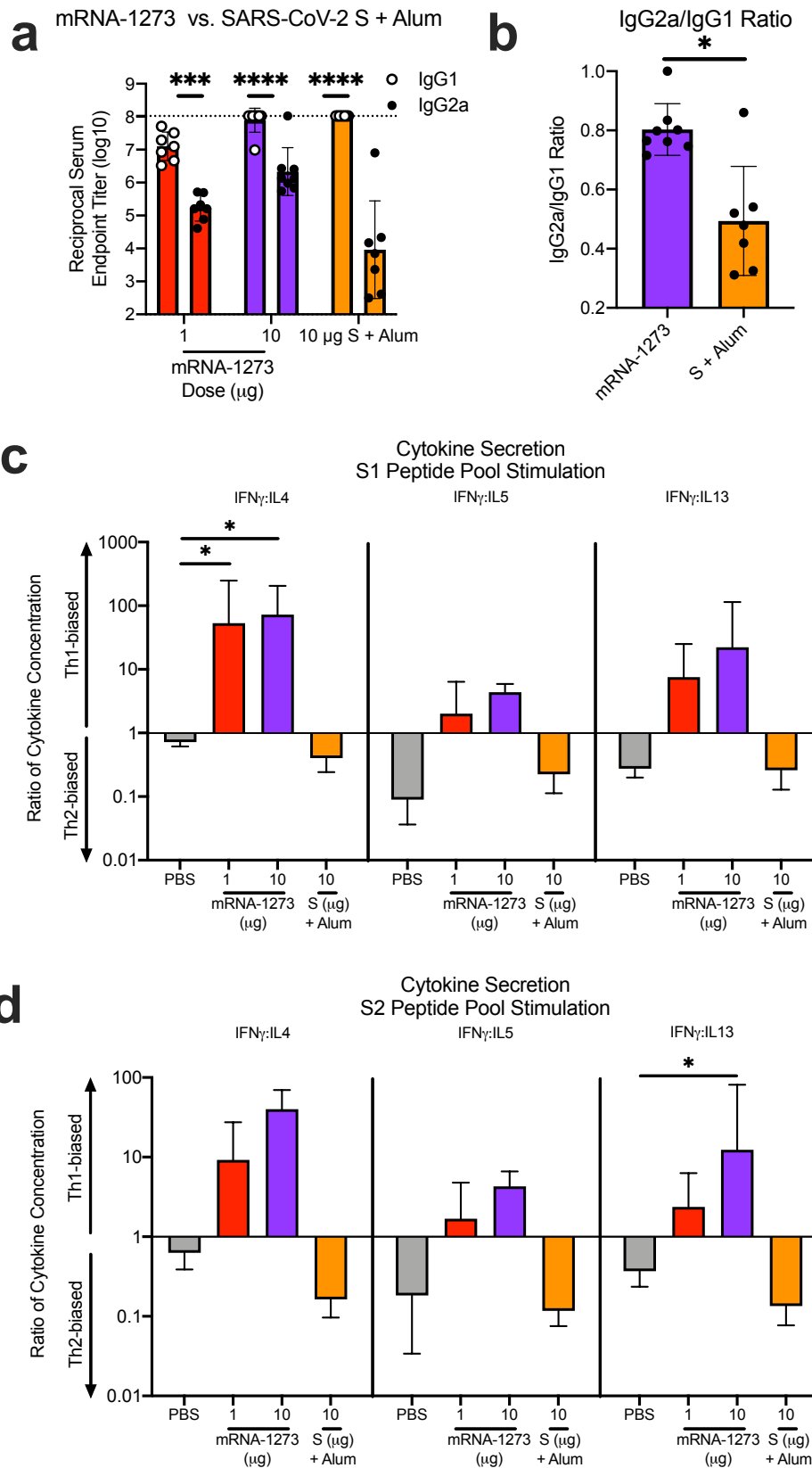**Extended Data Figure 5**. **A single dose of mRNA-1273 elicits robust antibody responses.**
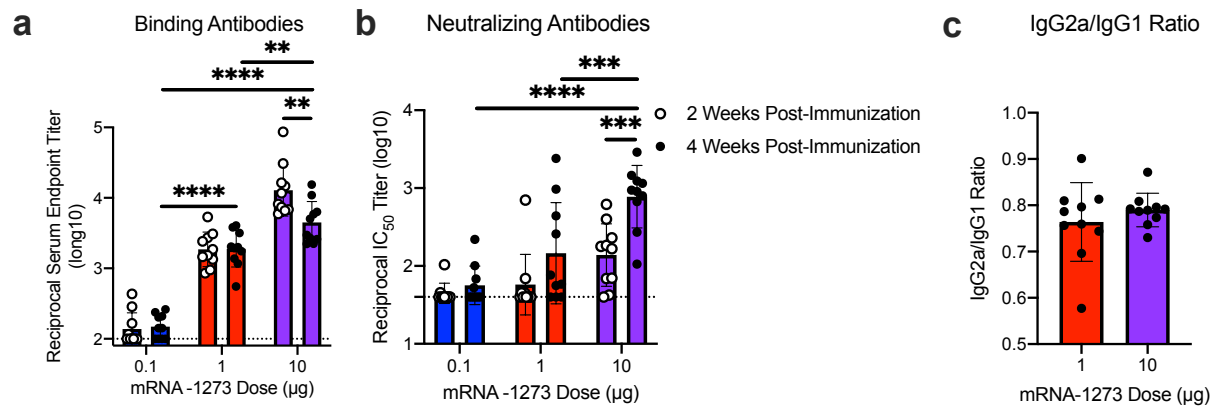
BALB/cJ mice were immunized with 0.1 (blue), 1 µg (red), or 10 µg (purple) of mRNA-1273. Sera were collected 2 (open circles) and 4 (closed circles) weeks post-immunization and assessed for SARS-CoV-2 S-specific total IgG by ELISA (a) and neutralizing antibodies against homotypic SARS-CoV-2 pseudovirus (b). (c) S-specific IgG2a and IgG1 were also measured by ELISA, and IgG2a to IgG1 subclass ratios were calculated. Dotted line = assay limit of detection. (a-b) Doses were compared 4 weeks post-boost, and timepoints were compared within each dose level.

Extended Data Figure 6. mRNA-1273 and SAS-adjuvanted S-2P protein elicit both IgG2a and IgG1 subclass S-binding antibodies. BALB/cJ (a-c) or C57BL/6J (d-f) mice were immunized at weeks 0 and 3 with 0.01 (green), 0.1 (blue), or 1 µg (red) of mRNA-1273 SARS-CoV-2 S-2P protein adjuvanted with SAS. Sera were collected 2 weeks post-boost and assessed by ELISA for SARS-CoV-2 S-specific IgG1 and IgG2a or IgG2c for BALB/cJ and C57BL/6J mice, respectively. Endpoint titers (a-b, d-e) and endpoint titer ratios of IgG2a to IgG1 (c) and IgG2c to IgG1 (f) were calculated. For mice for which endpoint titers did not reach the lower limit of detection (dotted line), ratios were not calculated (N/A). IgG1 and IgG2a/c (a-b, d-e) and immunogens (c, f) were compared at each dose level.
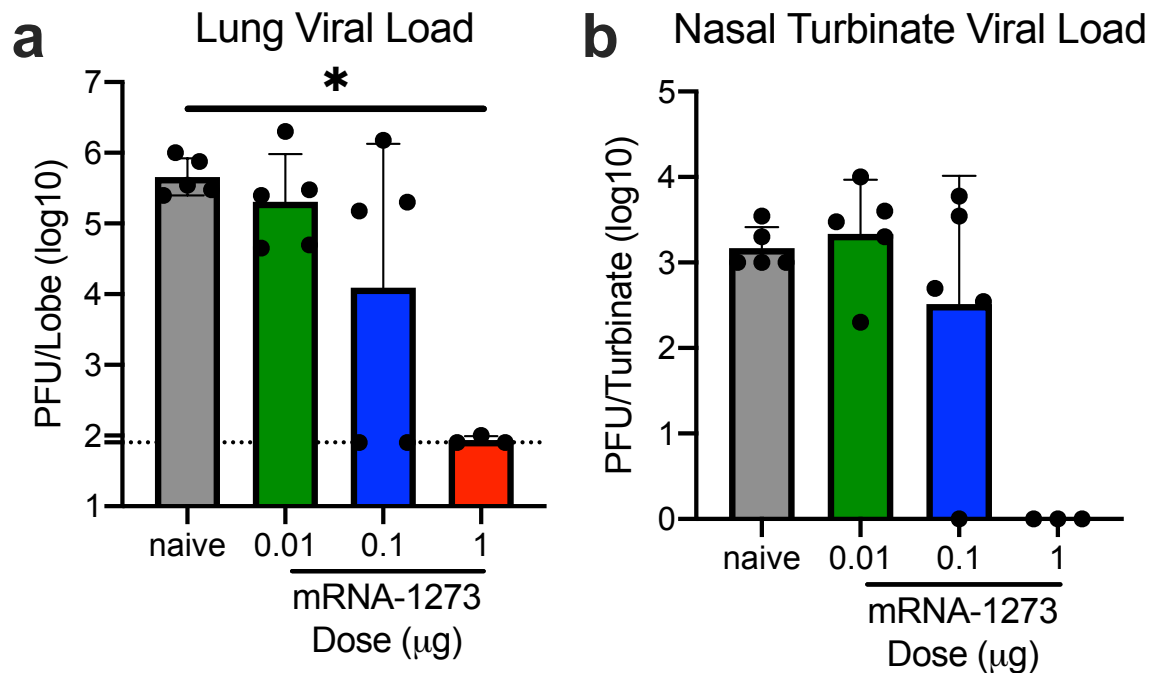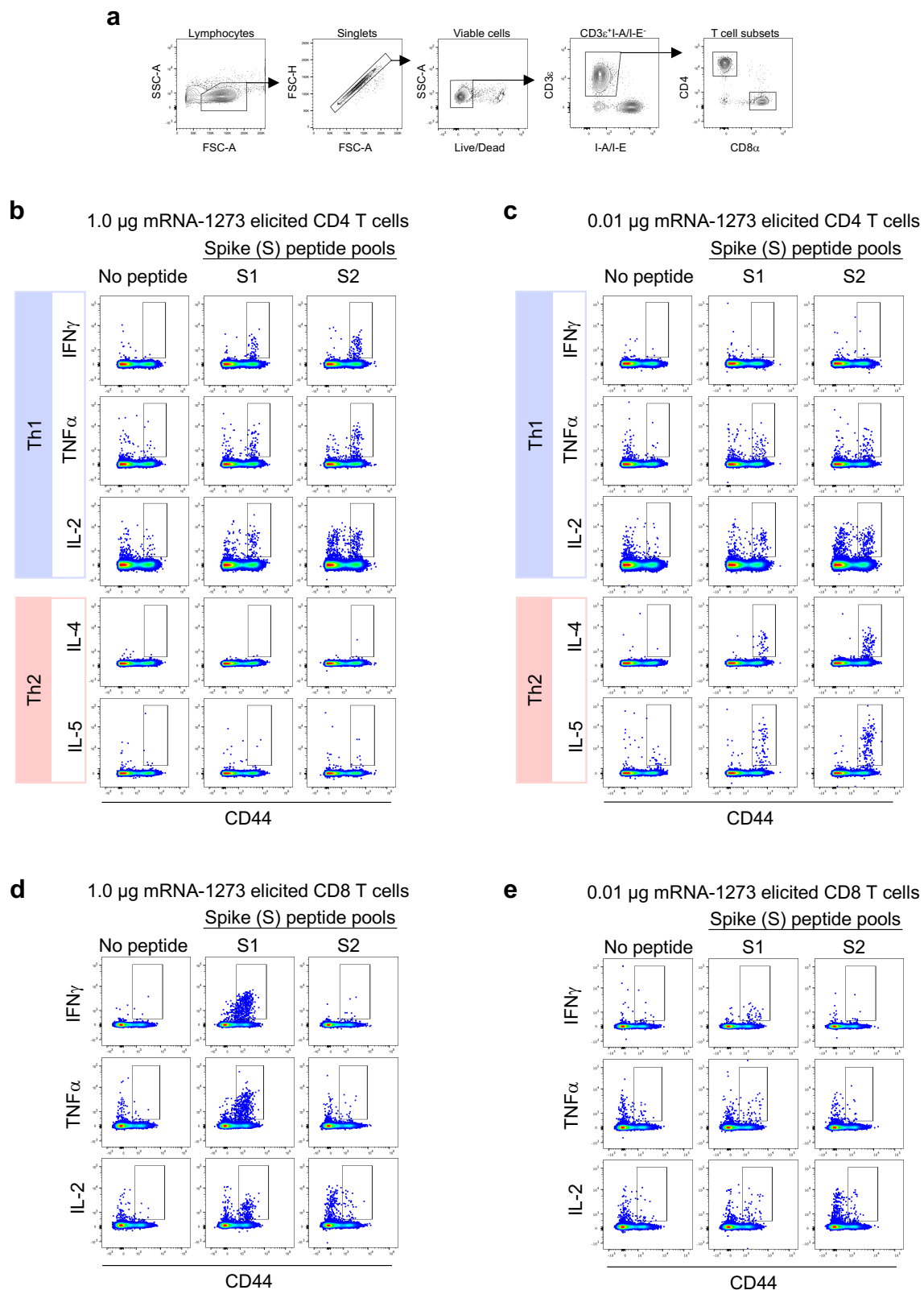
Extended Data Figure 7. **mRNA-1273 elicits Th1-skewed responses compared to S protein adjuvanted with alum.** BALB/c mice were immunized at weeks 0 and 2 weeks with 1 (red) or 10 µg (purple) of mRNA-1273 or 10 µg of SARS-CoV-2 S protein adjuvanted with alum hydrogel (orange). (a-b) Sera were collected 2 weeks post-boost and assessed by ELISA for SARS-CoV-2 S-specific IgG1 and IgG2a. Endpoint titers (a) and endpoint titer ratios of IgG2a to IgG1 (b) were calculated. (c-d) Splenocytes were also collected 4 weeks post-boost to evaluate IFN-γ IL-4, IL-5, and IL-13 cytokine levels secreted by T cells re-stimulated with S1 (c) and S2 (d) peptide pools, measured by Luminex. Dotted line = assay limit of detection. IgG1 and IgG2a/c (a) were compared at each dose level. (c-d) For cytokines, all comparisons were compared to PBS-immunized mice.

Extended Data Figure 8. **mRNA-1273 protects mice from upper and lower airway SARS-CoV-2 infection, 13 weeks post-boost.** BALB/cJ mice were immunized at weeks 0 and 3 with 0.01 (green), 0.1 (blue), or 1 µg (red) of mRNA-1273. Age-matched naive mice (gray) served as controls. Thirteen weeks post-boost, mice were challenged with mouse-adapted SARS-CoV-2. Two days post-challenge, at peak viral load, mouse lungs (a) and nasal turbinates (b) were harvested from 5 mice per group for analysis of viral titers. Dotted line = assay limit of detection. All dose levels were compared.

Extended Data Figure 9. **Flow cytometry panel to quantify SARS-CoV-2 S-specific T cells in mice.** (a) A hierarchical gating strategy was used to unambiguously identify single, viable CD4+ and CD8+ T cells. Gating summary of SARS-CoV-2 S-specific (b-c) CD4 (b-c) and (d-e) CD8 (d-e) T cells elicited by 1.0 and 0.01 µg mRNA-1273 immunization. Antigen-specific T cell responses following peptide pool re-stimulation were defined as CD44^{hi}/cytokine^{+}. Concatenated files shown were generated using the same number of randomly selected events from each animal across the different stimulation conditions using FlowJo software, v1

Extended Data Table 1. Concordance of Pseudovirus Neutralization Assay and PRNT.

Mouse Serum Pool #[1]	Reciprocal IC_{50} Titer		Fold Difference[4]
	Pseudovirus Neutralization[2]	PRNT[3]	
1	893.5 +/- 1.4	933.5	1.0
2	211.6 +/- 1.5	314.5	0.7
3	159.8 +/- 1.3	397.1	0.5

[1]BALB/cJ mice were immunized at weeks 0 and 3 with 1 µg SARS-CoV-2 S-2P protein, adjuvanted with SAS. Sera were collected 2 weeks post-boost and pooled (N = 3 mice/pool).

[2]IC_{50} titers were averaged from pseudovirus neutralization assays completed in 5 experimental replicates. (GMT +/- geometric SD)

[3]IC_{50} titer from PRNT assay completed once.

[4]Fold difference calculated as average pseudovirus neutralization IC_{50} titer relative to PRNT IC_{50} titer.